Site-specific characterization of threonine, serine, and tyrosine glycosylations of amyloid precursor protein/amyloid β-peptides in human cerebrospinal fluid

Adnan Halim[a,1], Gunnar Brinkmalm[b,1], Ulla Rüetschi[a], Ann Westman-Brinkmalm[b], Erik Portelius[b], Henrik Zetterberg[b], Kaj Blennow[b], Göran Larson[a,2], and Jonas Nilsson[a,2]

[a]Department of Clinical Chemistry and Transfusion Medicine, Institute of Biomedicine, University of Gothenburg, SE-413 45 Gothenburg, Sweden; and [b]Department of Psychiatry and Neurochemistry, Institute of Neuroscience and Physiology, University of Gothenburg, SE-431 80 Mölndal, Sweden

The proteolytic processing of human amyloid precursor protein (APP) into shorter aggregating amyloid β (Aβ)-peptides, e.g., Aβ1-42, is considered a critical step in the pathogenesis of Alzheimer's disease (AD). Although APP is a well-known membrane glycoprotein carrying both N- and O-glycans, nothing is known about the occurrence of released APP/Aβ glycopeptides in cerebrospinal fluid (CSF). We used the 6E10 antibody and immunopurified Aβ peptides and glycopeptides from CSF samples and then liquid chromatography—tandem mass spectrometry for structural analysis using collision-induced dissociation and electron capture dissociation. In addition to 33 unglycosylated APP/Aβ peptides, we identified 37 APP/Aβ glycopeptides with sialylated core 1 like O-glycans attached to Thr(−39, −21, −20, and −13), in a series of APP/AβX-15 glycopeptides, where X was −63, −57, −52, and −45, in relation to Asp1 of the Aβ sequence. Unexpectedly, we also identified a series of 27 glycopeptides, the Aβ1-X series, where X was 20 (DAEFRHDSGYEVHHQKLVFF), 19, 18, 17, 16, and 15, which were all uniquely glycosylated on Tyr10. The Tyr10 linked O-glycans were $(Neu5Ac)_{1-2}Hex(Neu5Ac)HexNAc$-$O$- structures with the disialylated terminals occasionally O-acetylated or lactonized, indicating a terminal Neu5Acα2,8Neu5Ac linkage. We could not detect any glycosylation of the Aβ1-38/40/42 isoforms. We observed an increase of up to 2.5 times of Tyr10 glycosylated Aβ peptides in CSF in six AD patients compared to seven non-AD patients. APP/Aβ sialylated O-glycans, including that of a Tyr residue, the first in a mammalian protein, may modulate APP processing, inhibiting the amyloidogenic pathway associated with AD.

Alzheimer's disease | glycoproteomics | O-glycosylation | sialic acid | biomarker

The amyloid precursor protein (APP) is a ubiquitously expressed type 1 transmembrane glycoprotein (1–3). Although much has been learned about proteolytic processing of APP into smaller peptides (4–6), a process critical for the pathogenesis of Alzheimer's disease (AD), very little attention had been paid to the biological effects of glycosylation of APP. Thus, since the pioneering structural work by Spitalnik and coworkers on APP glycosylation and secretion (1, 7) additional glycoproteomic data has not appeared until recently when Perdivara et al. defined three Thr linked O-glycan attachment sites of APP (2). Our approach has been to investigate whether any APP-derived glycopeptides may be identified in human cerebrospinal fluid (CSF), a body fluid that because of its proximity to the brain parenchyma provides diagnostic biomarkers—e.g., amyloid β (Aβ) 1-42, Tau, and phosphorylated Tau (8)—not only to track progression of AD but potentially to suggest diagnosis in presymptomatic stages. CSF samples thus offer insight into otherwise inaccessible processes in AD patients (9) and could give us valuable clues as to how glycosylation may affect the proteolytic processing of APP especially in relation to the early progression of AD. The processing of APP is of particular importance because variations in both the N- and C-terminal regions of the Aβ peptides in CSF may

have physiological and pathological significance. AD is a complex progressive neurodegenerative disease, which clinically starts with mild cognitive impairment and ends with severe dementia, and for which there is presently no cure. The AD-affected brain is characterized by amyloid plaques and neurofibrillar tangles (originally described by Alois Alzheimer in 1906 as miliary bodies and dense bundles of fibrils), which contain aggregated Aβ peptides (10) and hyperphosphorylated forms of the tau protein (11), respectively. The Aβ peptides and tau proteins are now in clinical use as biomarkers of AD, but additional biomarkers are needed to increase the diagnostic sensitivity and specificity for early diagnosis (9). The membrane bound APP is known to undergo proteolysis by several secretases in the processes of ectodomain shedding and regulated intramembrane proteolysis (12). In the amyloidogenic pathway β- and γ-secretases cleave APP into several Aβ isoforms (*SI Appendix*, Fig. S1) of which the 42 amino acid isoform (Aβ1-42) is one of the major constituents of amyloid plaques in the brains of AD patients (13). APP may also be cleaved in the middle of the Aβ1-42 sequence by α-secretase, precluding the formation of Aβ1-42 and thus considered to protect from amyloid deposition in the brain (9). Furthermore, it is believed that clearance of Aβ by the action of peptidases may counteract amyloid buildup (14–16). An impairment in this process may be an important component in the pathogenesis of sporadic AD (17). The proteolytic destiny and lifetime of some other glycoproteins are governed by O-glycosylations, which change the accessibility of the proteolytic sites (18, 19). Three O-glycosylation sites of APP have so far been described (2), but it is not known whether any glycans are positioned in the immediate vicinity to or even within the Aβ sequence itself. To address the site-specific O-glycosylation of APP we immunopurified APP/Aβ peptides from human CSF using antibody 6E10 (specific for Aβ amino acid residues ∼4–9) and then analyzed the enriched peptides and glycopeptides directly by liquid chromatography (LC)—tandem mass spectrometry (LC-MS^n).

Results

Copurification and Relative Amounts of Aβ Peptides and Glycopeptides in CSF. A typical total ion current chromatogram of a 6E10 immunopurified CSF sample is shown in *SI Appendix*, Fig. S2A.

All the major peaks were identified as multiple charged ions of previously described Aβ peptides in CSF (20, 21) with a dominance of the Aβ1-40 and Aβ1-38 isoforms. Altogether 33 different Aβ peptides were identified (*SI Appendix*, Table S1) some of which, e.g., Aβ1-15, previously identified as a positive biomarker of γ-secretase inhibition (22, 23), constituted less than 1% of the total ion current chromatogram. No sign of any glycosylated derivatives of Aβ1-40 (*SI Appendix*, Fig. S2B) nor of Aβ1-38 and Aβ1-42 was detected in the mass spectra. However, coeluting with Aβ1-15 (*SI Appendix*, Fig. S2C), ions matching Aβ1-15 with an additional mass shift corresponding to di- and trisialylated Hex-HexNAc derivatives (SA$_2$-Aβ1-15 and SA$_3$-Aβ1-15, respectively) were observed. The relative amounts of glycosylated versus unglycosylated Aβ1-15 peptides were determined and was found to be about 10%. Altogether 64 glycopeptides belonging to the APP/AβX-15 and Aβ1-*X* series (*SI Appendix*, Fig. S1) were identified in CSF and their relative amounts versus their unglycosylated counterparts were measured (*SI Appendix*, Table S1).

O-glycosylation of Aβ1-*X* Peptides in CSF. Analysis of fragment spectra (MS^2) induced by collision-induced dissociation (CID) confirmed the sequence of Aβ1-15, 1-16, 1-17, 1-40, and 1-42 (21, 24). By specifically searching for glycosidic fragmentation patterns in the MS^2 and MS^3 (second generation fragment) spectra we were able to identify O-glycosylated Aβ1-15, 1-16, 1-17, 1-18, 1-19, and 1-20 (Aβ1-*X* series) as well as Aβ−3-15, 4-15, 4-17, and 5-17 peptides, also included in the Aβ1-*X* series, with an additional mass and structure corresponding to a Neu5AcHex(Neu5Ac)HexNAc-*O*- (SA$_2$) glycan within each of the peptides (Fig. 1A, *SI Appendix*, Fig. S3, Table S1). We also identified trisialylated glycoforms with a terminal disialosyl structure, Neu5AcNeu5AcHex(Neu5Ac)HexNAc-*O*- (SA$_3$) glycan (Fig. 1B), which occasionally was derivatized with a Neu5Ac O-acetyl group (*O*-AcSA$_3$) (Fig. 1C). Initial loss of O-AcNeu5Ac but not of Neu5Ac or Hex demonstrated that the O-acetyl group was attached to the terminal sialic acid of the disialosyl group. Further CID MS^3 fragmentation at the mass-to-charge ratio (m/z) 694.4 showed that one Neu5Ac was attached to the Hex-NAc because a peptide + Neu5AcHexNAc peak at m/z 774.6 was observed (Fig. 1C, *Right*). We also observed lactone formation between the two terminal sialic acids, which is typical for the Neu5Acα2,8Neu5Ac linkage, suggesting that these two residues were linked via an α2,8 glycosidic bond (25) (Fig. 1 D and E). Analysis of the MS^2 spectrum of the lactonized SA$_3$-Aβ4-15 gly-copeptide showed that the disialosyl structure was linked to the Hex and not to the HexNAc residue (*SI Appendix*, Fig. S3C). For monosialylated Aβ1-*X* glycopeptides, which were minor components, we found that the sialic acid was only attached to the Hex residue (*SI Appendix*, Fig. S3 A and G).

In total, we analyzed more than 50 CSF samples including six samples from AD patients and seven from non-AD patients and identified O-glycosylated Aβ1-15 and Aβ1-17 peptides, the most abundant of all Aβ1-*X* glycopeptides, in all the samples. In contrast, we did not detect any glycosylated Aβ1-28, 1-30, 1-33, 1-34, 1-37, 1-38, 1-39, 1-40, or 1-42 peptides in any of the samples even though all the unglycosylated peptides were present in the mass spectra, and Aβ1-40 and 1-38 are among the dominating Aβ isoforms in CSF (*SI Appendix*, Fig. S2A). Altogether, we identified 27 Aβ1-*X* glycopeptides from 10 Aβ1-*X* isoforms.

Quantitation of Aβ1-15 Peptide and Glycopeptides in CSF. To estimate the absolute concentrations of Aβ1-15 and its glycosylated counterparts, we added an isotopically labeled Aβ1-15-Arg-^{13}C^{15}N peptide (Aβ1-15*) to CSF samples before immunopurification (n = 6). On the simplified assumption that all Aβ1-15 isoforms were enriched and ionized equally well, the sum of the concentrations of all Aβ1-15 glycoforms was calculated to be 10–30 pg/mL whereas the unglycosylated Aβ1-15 isoform alone was in the
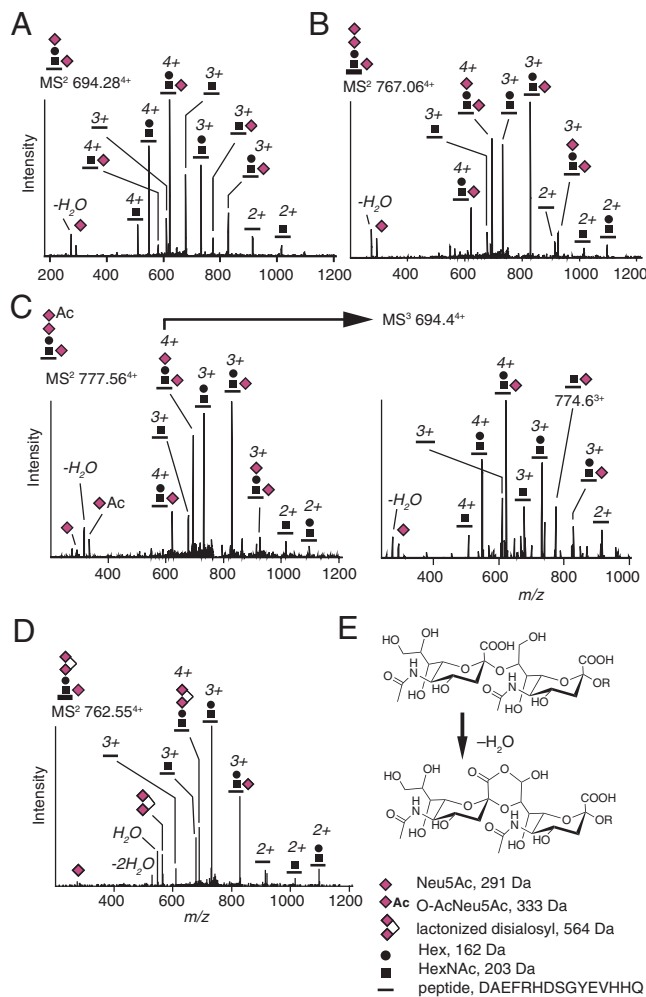

Fig. 1. Glycosylated and sialylated Aβ1-15 peptides from human CSF. CID MS^2 spectra of (A) SA$_2$-Aβ1-15 and (B) SA$_3$-Aβ1-15. (C) O-AcSA$_3$-Aβ1-15 (*Left*) with MS^3 fragmentation at m/z 694.4 (*Right*), and (D) lactonized SA$_3$-Aβ1-15. (E) Structure of α2,8-linked disialic acid terminal and its lactonized form. The Neu5Ac oxonium ion and its loss of H$_2$O are present at m/z 292 and 274, respectively. Neu5Ac, *N*-acetyl-5-neuraminic acid; Hex, hexose; HexNAc, *N*-acetylhexosamine; O-Ac, O-acetyl.

range 100–200 pg/mL for the different samples (*SI Appendix*, Fig. S2D).

Tyrosine Glycosylation and Sialylation of Aβ1-*X* Peptides in CSF. To confirm the peptide sequences and pinpoint the glycosylation site of Aβ1-*X* glycopeptides we used electron capture dissociation (ECD) to induce peptide backbone fragmentation in the presence of intact O-linked glycans (26). To our surprise, the ECD spectra of Aβ1-15 and Aβ1-17 glycopeptides demonstrated unequivocally that the glycan was selectively attached to Tyr10 of the Aβ sequence (Fig. 2). The presence of unglycosylated *c*8 ions (DAEFRHDS, m/z 975.43) and *c*9 ions (DAEFRHDSG, m/z 1,032.45) showed that Ser8, the anticipated attachment site, was not glycosylated whereas *c*10-*c*14 ions, containing the Tyr10 residue, included the mass of the SA$_2$ glycan (Fig. 2 A and B, respectively) or the SA$_3$ glycan (*SI Appendix*, Fig. S4 E and F, respectively). For SA$_2$-Aβ1-15 we detected a peak corresponding to the *z*6 ion (YEVHHQ) that included the mass of the glycan but excluded the Ser8 residue (m/z 872.35, Fig. 2A). Analogously, for SA$_2$-Aβ1-17 we observed *z*8 (YEVHHQKL, m/z 992.94) and *z*9 ions (GYEVHHQKL, m/z 1,021.44) that included a Tyr10 glycosylation (Fig. 2B). The peaks of the *z*8 and *M-Ac* (m/z 991.77) ions were coinciding but the distinguishable presence of the *z*8
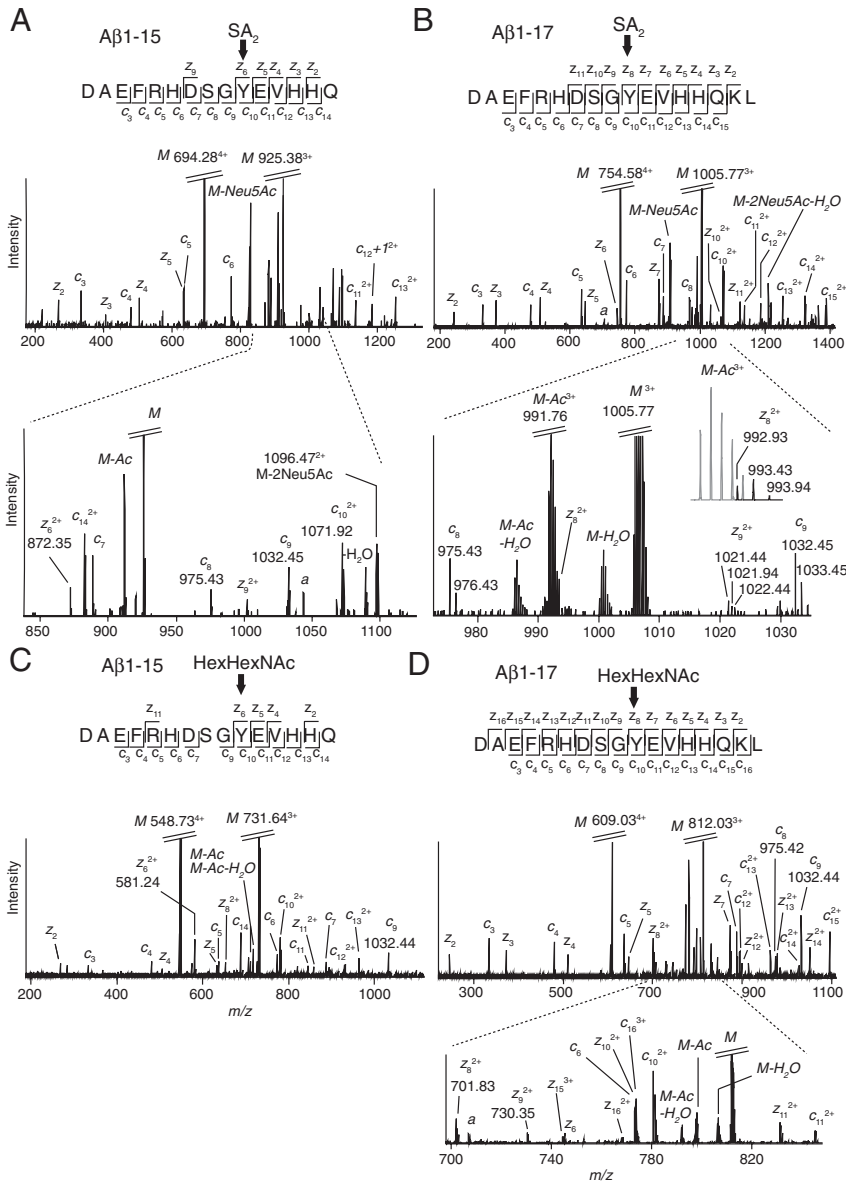
Fig. 2. ECD MS^2 fragmentation spectra of Aβ1-15 and Aβ1-17 glycopeptides. ECD spectra of (*A*) SA_2-Aβ1-15, including an *m/z* expansion showing the $z6$, $c8$, and $c9$ fragments. (*B*) SA_2-Aβ1-17, with an *m/z* expansion showing the $z8$ and $z9$ fragments. The isotopic peaks of the $z8$ fragment are resolved in the *Inset*. (*C*) HexHexNAc-Aβ1-15. (*D*) HexHexNAc-Aβ1-17 including an *m/z* expansion showing the $z8$ and $z9$ fragments. Parent ions (*M*) and the charged-reduced forms were base peaks and were cropped. Noise peaks are denoted as *a*. Fully *m/z* annotated ECD spectra and lists of *c*- and *z*-ions for all observed Tyr10 glycosylated Aβ1-*X* peptides are shown in *SI Appendix*, Fig. S4 *A–K*.

isotopes are demonstrated in the *Inset*. To further verify the identities of the glycosylated *z*-ions we treated 6E10 immunopurified CSF samples with 0.1 M formic acid at 80 °C to selectively hydrolyze sialic acid glycosidic bonds (27) and transform all SA_2 and SA_3 glycans into a HexHexNAc-*O*- glycan and thus induce predictable mass-shifts for the critical *z*-ions. For HexHexNAc-Aβ1-15 the $z6$ ion had now shifted to *m/z* 581.24, corresponding to the exact loss of two Neu5Ac, and appeared as one of the most prominent fragment ions (Fig. 2*C*). In the ECD spectrum of HexHexNAc-Aβ1-17 (Fig. 2*D*) all possible *c*- and *z*-ions could now be identified, including glycosylated $z8$ at *m/z* 701.83, which was no longer partially concealed, and glycosylated $z9$ at *m/z* 730.35 thus once again giving evidence for Tyr10 as the site of glycosylation.

For all peptide backbone fragment ions including the Tyr10 residue, we observed only completely glycosylated ions and no further fragmentation events into partially or totally unglycosylated *c*- or *z*-ions, such as those found for the Aβ1-15 peptide (*SI Appendix*, Fig. S4*G*). We observed only sparse glycosidic fragmentation of Neu5Ac or loss of acetyl groups from charge-reduced parent ions in the ECD spectra. Additional ECD spectra of Aβ1-*X* glycopeptides, all in support of Tyr10 glycosyla-

tion, are presented in *SI Appendix*, Fig. S4 *E–K*. CSF samples from both AD ($n = 3$) and non-AD patients ($n = 3$) were used in the ECD experiments, and for all samples Tyr10 was confirmed as the glycosylation site.

Increased Amounts of Aβ1-*X* Glycopeptides in CSF from AD Versus Non-AD Patients. In a pilot study of CSF samples from AD patients ($n = 6$) and non-AD patients ($n = 7$) we observed that the mean relative abundance of the most abundant Tyr10 glycosylated versus all unglycosylated Aβ peptides (Aβ1-42 excluded) was increased by a factor of 1.1 to 2.5 for the AD patients (Fig. 3 and *SI Appendix*, Table S1). The mean intensity ratios of each of the Aβ glycopeptides versus their corresponding unglycosylated peptides were also generally higher for AD compared to non-AD patients for most of the Aβ1-*X* series (*SI Appendix*, Fig. S9).

O-glycosylation of APP/Aβ*X*-15 Peptides in CSF. In addition to the series of Tyr10 glycosylated Aβ1-*X* peptides, we identified a series of O-glycosylated APP/Aβ*X*-15 peptides in CSF (Fig. 4, *SI Appendix*, Fig. S1, Fig. S5, Table S1). The ECD spectrum of glycosylated APP/Aβ−25-15 showed that a single Neu5AcHex (Neu5Ac)HexNAc-*O*- glycan was attached to either Thr(−21) or
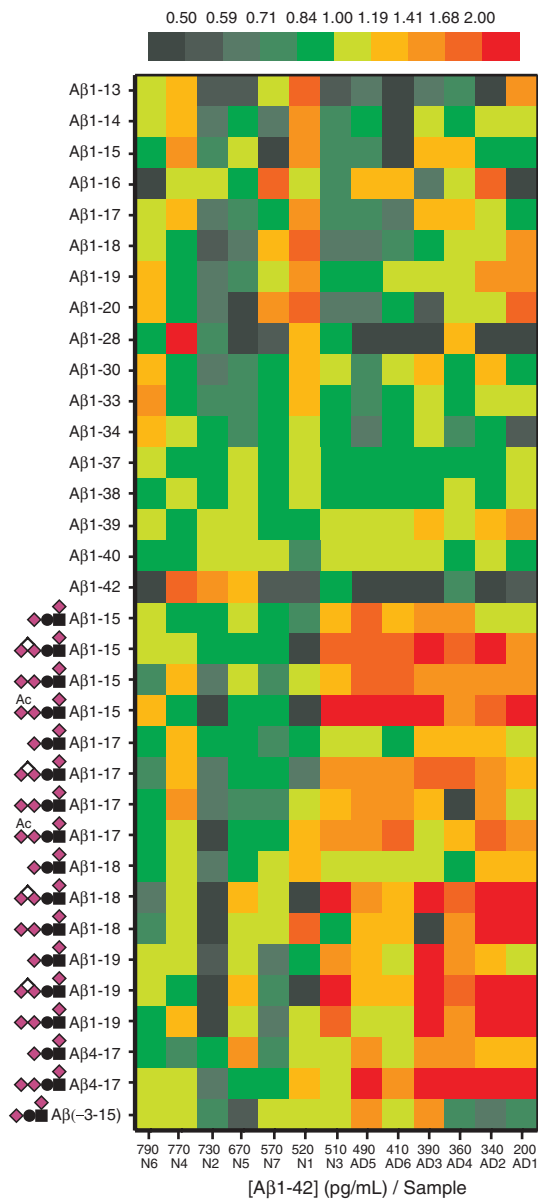
Fig. 3. Heatmap for the relative signal intensities of individual Aβ1-X peptides and glycopeptides for Alzheimer (AD1-6) and non-Alzheimer (N1-7) patients. The samples are arranged according to their Aβ1-42 concentrations. An increase of Tyr10 glycosylated Aβ peptides for AD patients is seen as a red shift.

Fig. 4. MS^1 and CID MS^2 of APP/AβX-15 glycopeptides. (A) Amino acid sequence of APP/AβX-15, where X = −63, −57, −51, and −25. Underlined residues show Thr(−39, −21, −20, and −13) glycosylation sites. Either Ser(−5) or Thr(−9) was glycosylated (dashed underlines). The b9, b15, b21, and y57 fragmentation site is indicated. (B) CID MS^2 of triglycosylated APP/Aβ−25-15 showing neutral loss of Neu5Ac from the glycopeptide. (C) Triglycosylated APP/Aβ−51-15 with diagnostic b9 (m/z 987.4) and glycosylated y57 fragment ions. (D) Triglycosylated APP/Aβ−57-15 with diagnostic b15 (m/z 835.0) and glycosylated y57 fragments. (E) Tetraglycosylated APP/Aβ−63-15 with a diagnostic b21 fragment (m/z 1,151.5).

Thr(−20) as opposed to Tyr10 (*SI Appendix*, Fig. S6). The molecular masses of parent ions and CID MS^2 glycosidic fragmentation patterns corresponded to one Neu5AcHex(Neu5Ac) HexNAc-O- and/or one to four Neu5AcHexHexNAc-O- glycans within each of the APP/AβX-15 glycopeptides. The identities of the APP/Aβ−63-15, −57-15, −51-15, and −45-15 glycopeptides were confirmed by the presence of signature peptide fragment ions in the CID MS^2 spectra (Fig. 4 and *SI Appendix*, Fig. S5).

With capture-and-release enrichment (27) on 6E10 immunopurified CSF samples and directly on peptide N-glycosidase F-treated CSF samples (in preparation), we identified tryptic glycopeptides with one to three O-glycans attached in the −21-(−13) region (*SI Appendix*, Fig. S7). The glycopeptide with three separate glycans was the most abundant and the ECD spectrum showed that Thr (−21, −20, and −13) were all glycosylated (*SI Appendix*, Fig. S7A). We also identified one glycosylation site
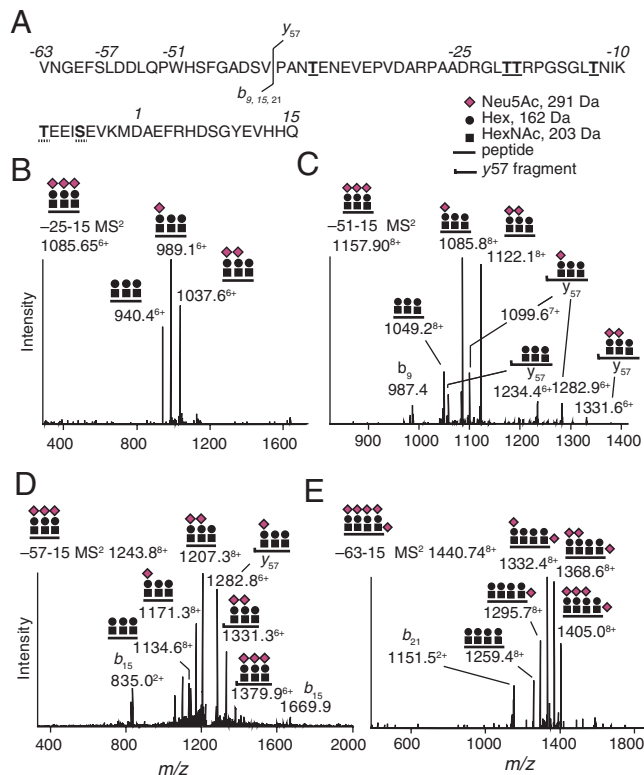
residing on either Ser(−5) or Thr(−9), and one on Thr(−39) (*SI Appendix*, Fig. S8).

We were not able to detect any glycopeptides with O-glycosylations of both the Thr/Ser and Tyr residues (see *SI Appendix*, Fig. S6) indicating that Tyr10 was not glycosylated on the APP/AβX-15 glycopeptides. O-linked glycans on Thr (−39, −21, −20, and −13), and on Ser(−5)/Thr(−9) accounted for up to five separate glycans on the APP/AβX-15 series without terminal disialosyl structures, O-acetylation or lactonization. The APP/Aβ−51-15 glycopeptides typically constituted >90% of all measurable APP/Aβ−51-15 species whereas the APP/Aβ−25-15 glycopeptides were minor components (<10%) compared to the unglycosylated isoform (*SI Appendix*, Fig. S9). We did not observe any obvious changes in relative amounts of glycosylated or unglycosylated APP/AβX-15 peptides for the AD versus non-AD patients (*SI Appendix*, Fig. S10, Table S1).

Discussion

In this report we have uniquely identified O-glycosylated APP/Aβ amyloid peptides in human CSF samples, including glycosylation of a Tyr residue. The relative amounts of the SA$_2$-Aβ1-15 glycopeptide, one of the most abundant of the Aβ glycopeptides identified in CSF, was approximately 10% of the unglycosylated Aβ1-15 peptide (10–30 pg/mL versus 100–200 pg/mL, measured by LC-MS using isotopically labeled Aβ1-15 peptide), which in turn was less than 1% of the most abundant Aβ1−38/40 peptides in CSF. As a comparison, the concentrations of Aβ1-42 peptide in individual samples were in the range of 200–800 pg/mL. For some less abundant Aβ peptides the glycosylated peptides out-

BIOCHEMISTRY

CHEMISTRY

numbered the unglycosylated isoforms by a factor of 10 to 100 whereas for others the reverse was true. These relative differences in peptide concentrations may reflect differences in processing and degradation of differentially glycosylated APP and Aβ isoforms.

Despite the low amounts of APP/Aβ glycopeptides the LC-MS^n analysis revealed 64 unique glycopeptides and their O-glycan structures and in several cases their exact attachment sites. The analysis also revealed a hitherto unknown complex glycosylation of a tyrosine residue (Tyr10). Tyrosine residues are well-known to become phosphorylated or sulfated, but glycosylation of the Tyr hydroxyl group has only been described for glucosylation of glycogenin (28, 29), and in some prokaryotic glycoproteins (30). The unique Tyr10 glycosylation thus adds another amino acid to the well-known Ser and Thr residues as possible O-glycan attachment sites for sialylated glycans on mammalian proteins.

Due to the inherent complexity of glycan isomers, no single analysis—not even the high resolution and sensitive LC-MS^n used here—will give all structural information needed to pinpoint the monosaccharide identities, their sequence, saccharide linkage positions, and anomeric configurations. Thus HexNAc could be GlcNAc, GalNAc, or even ManNAc and in either α- or β-linkage to the conjugated amino acid. Similarly, Hex could be Gal, Man, or Glc, etc. However, it is most likely that the glycan Neu5AcHex (Neu5Ac)HexNAc-O-Ser/Thr that we describe for the APP/AβX-15 series of glycopeptides is identical to the disialylated core 1 structure Neu5Acα3Galβ3(Neu5Acα6)GalNAcα1-O-Ser/Thr earlier identified from released O-glycans of APP (1). For the Tyr10 glycans of the Aβ1-X series, on the other hand, it is not obvious that they are identical to the core 1 structure. Because Tyr represents a unique attachment site, the innermost HexNAc may not be the common GalNAcα-linked residue and an alternative glycosyltransferase may then be responsible for catalyzing the Tyr O-glycosylation. On the other hand, there are now 20 human GalNAcα-glycosyltransferases cloned and functionally expressed (31) and perhaps one or two of them, with preference for expression in neuronal tissues, might glycosylate this unique Tyr residue of APP. A core 1 trisialylated structure Neu5Acα8-Neu5Acα3Galβ3(Neu5Acα6)GalNAc, similar to the SA$_3$ glycan that we have now described, was indeed reported to be a minor glycan (<5%) released from glycophorin B of red blood cells (32), and from von Willebrand factor (33).

The Tyr10 sialylated structures observed for Aβ1-X glycopeptides are analogous to the terminal disialylated structures found on brain gangliosides GD1c, GT1a, and GQ1b. Structural changes of brain gangliosides in AD patients and transgenic mice models of human AD have been the object of detailed studies (34, 35) because gangliosides are implied to function in axonal regeneration (36). Although there are regional differences, the general trend in AD brains is a loss of complex gangliosides, but the functional significance of such changes is presently difficult to translate into AD pathogenesis. The disialylated terminals of the Aβ1-X series of glycopeptides are interesting because in some unique cases sialic acids are linked to each other into long polysialic acid chains of repetitive Neu5Acα2,8Neu5Ac structures. Such polysialic acid chains have been found for instance on polysialoglycoprotein (PSGP) of fish eggs (37), neural cell adhesion molecule (NCAM), and synaptic cell adhesion molecule 1 (SynCAM1) in the mammalian brain (38, 39). The expression of the polysialic acids of NCAM in the brain is temporally and spatially regulated during neural development (40) and plays important roles in cell migration, neurite outgrowth, neuronal recognition, and synaptogenesis (41). The polysialic acid chains of NCAM and SynCAM1 are N-linked, whereas those of PSGP are O-linked. The possibility of finding polysialylated O-linked glycans on APP molecules is challenging and warrants further studies, not only in humans but also in other species, cell lines, and in transgenic animals expressing human APP.

In a smaller series of CSF samples we found an increase of the dominating Tyr glycosylated versus unglycosylated Aβ1-X peptides in AD compared to non-AD patients. In contrast, we could not observe any obvious changes of relative concentrations for other series of Thr/Ser O-glycosylated or unglycosylated APP/AβX-15 peptides. The patients were divided into AD and non-AD groups on the basis of a combined CSF biomarker profile of Aβ1-42, total and phosphorylated tau that is 90% sensitive and specific for AD (8). However, the two groups are overlapping and for two of the non-AD patients the Aβ1-42 concentrations, being the earliest biomarker sign of AD (42), were below the AD cutoff level at 530 pg/mL, which may indicate early AD. At least for one of these (Fig. 3, N3) the glycopeptide profile was actually more similar to the AD patients. Obviously, the number of samples was limited, and to establish Aβ glycopeptides as clinically useful biomarkers the glycopeptide profiles and concentrations need to be confirmed in much larger prospective studies. Such studies may take advantage of the methodology and findings presented here.

The γ-secretase complex is known to cleave type 1 integral membrane proteins like APP and Notch in the process of regulated intramembrane proteolysis (43). Although very little is known on how glycosylation may alter such proteolysis it is not unlikely that multiple O-glycosylations of APP, as described here for the six glycosylation sites from Thr(−39) to Tyr10 just in the vicinity of the protease cleavage sites of APP, are important for the processing of this protein. Suppressive effects on proteolytic processing of proteins by selective O-glycosylations have been described for both soluble and membrane-bound glycoproteins such as angiopoietin-like protein 3 (ANGPTL3) (18), B-type (brain) natriuretic propeptide (19), low density lipoprotein receptors (44), and copper transporter hCTR1 (45). It is thus reasonable to believe that a large (~1 kDa) and negatively charged glycan (on, e.g., Tyr10) may substantially influence the mode upon which this region of APP can interact with various membrane components and influence cleavages by the α-, β-, and γ-secretases. We propose that in the presence of a Tyr10 O-glycosylation γ-secretase-dependent cleavage is modified, such that instead of cleavage at amino acid residues 40-42, the residues at 15-20 become the preferred cleavage sites (9, 46). This hypothesis is based on the presence and structures of the Aβ1-X series of Tyr10 O-glycosylated peptides (Aβ1-15, 1-16, 1-17, 1-18, 1-19, and 1-20) and the lack of glycosylated Aβ1-40/42 peptides in CSF. However, the appearance of Aβ peptides in CSF is the result of both complex production and clearance mechanisms (17). Further investigations are thus warranted to address the significance of Tyr10 glycosylation in the proteolysis of APP into various Aβ peptides and glycopeptides and their effects in amyloid deposition.

Materials and Methods

Ethical Consideration and CSF Sampling. CSF samples were supplied by the Clinical Neurochemistry Laboratory, Sahlgrenska University Hospital. The study was approved by the local ethical committees and conducted according to the Helsinki declaration. Samples were collected by lumbar puncture from patients who sought medical advice due to cognitive impairment. The first 10–12 mL of CSF were collected, centrifuged at 1,800 × g for 10 min, and stored at −80 °C before use. None of the patients had a family history of autosomal dominant forms of AD. Patients were designated as non-AD or AD according to conventional CSF biomarker levels using cutoffs that together are 90% sensitive and specific for AD (8): total tau (t-tau) >350 ng/L, phosphorylated tau (p-tau) >80 ng/L, and Aβ1-42 <530 ng/L. Detailed cognitive profiling was not available for the included subjects. None of the individuals were genotyped for presenilin or APP mutations, but the MS analysis did not give evidence for any amino acid mutations in the APP/Aβ sequences.

Purification of APP/Aβ Peptides and Glycopeptides from CSF. Immunopurification of Aβ peptides from CSF using the 6E10 antibody (2–10 μg antibody/mL of CSF, Signet Laboratories) was performed as described (20). Capture-and-release of sialylated glycopeptides was performed as published (27) with a few modifications. CSF (1.0 mL) or 6E10 immunopurified Aβ from 5 mL CSF, dissolved in 25 μL 20% acetonitrile in 0.1% formic acid (FA), were oxidized with periodic acid (2 mM) at 0 °C for 10 min. The samples were desalted with PD MidiTrap G-25 columns (GE Healthcare) and hydrazide magnetic beads (100 μL, Bioclone) were used for capture.

Mass Spectrometric Analysis. Nanoflow liquid chromatography (Ettan MDLC, GE Healthcare) coupled to electrospray ionization Fourier transform ion cyclotron resonance (LC-ESI-FTICR) on an LTQ-FT instrument (Thermo Fisher) was used. A nanoscale C4 column (150 × 0.075 mm, G&T Septech) and a linear gradient of 0–53% acetonitrile in 0.1% formic acid in water at 400 nL/min for 50 min were used. The CID energy was set to 30 and the ECD energy was set to 4–5 with 60–80 ms irradiation time. In one case (Fig. 2B), we used a multiple reaction monitoring approach with continuous ECD fragmentation at a fixed m/z value to increase sensitivity. In general the mass accuracy was <5 ppm for all precursor ions. Identification of peptides and glycopeptides was done by both Mascot database search and by manual analysis. For the quantitative AD study the LTQ-FT was set to acquire full scan spectra, and the DeCyder 2.0 application (GE Healthcare) was used for quantitative analysis. Masses and summed intensities of peaks for individual isoforms were obtained by deconvolution of all charge states during their elution into one peak. Peaks from individual LC-MS acquisitions were normalized to the summed intensities of all unglycosylated Aβ peptides except Aβ1-42 because its concentration is decreased in AD patient CSF (8). Normalized intensity values were further adjusted so that the average of individual unglycosylated Aβ became 1.0 for each of the non-AD patients.

1. Sato Y, et al. (1999) Study of the sugar chains of recombinant human amyloid precursor protein produced by Chinese hamster ovary cells. *Biochim Biophys Acta* 1472:344–358.
2. Perdivara I, et al. (2009) Elucidation of O-glycosylation structures of the beta-amyloid precursor protein by liquid chromatography-mass spectrometry using electron transfer dissociation and collision induced dissociation. *J Proteome Res* 8:631–642.
3. Akasaka-Manya K, et al. (2008) Increased bisecting and core-fucosylated N-glycans on mutant human amyloid precursor proteins. *Glycoconjugate J* 25:775–786.
4. Ahn K, et al. (2010) Activation and intrinsic {γ}-secretase activity of presenilin 1. *Proc Natl Acad Sci USA* 107:21435–21440.
5. De Strooper B, Vassar R, Golde T (2010) The secretases: Enzymes with therapeutic potential in Alzheimer disease. *Nat Rev Neurol* 6:99–107.
6. Sisodia SS (1992) Beta-amyloid precursor protein cleavage by a membrane-bound protease. *Proc Natl Acad Sci USA* 89:6075–6079.
7. Påhlsson P, Spitalnik SL (1996) The role of glycosylation in synthesis and secretion of beta-amyloid precursor protein by Chinese hamster ovary cells. *Arch Biochem Biophys* 331:177–186.
8. Hansson O, et al. (2006) Association between CSF biomarkers and incipient Alzheimer's disease in patients with mild cognitive impairment: A follow-up study. *Lancet Neurol* 5:228–234.
9. Blennow K, Hampel H, Weiner M, Zetterberg H (2010) Cerebrospinal fluid and plasma biomarkers in Alzheimer disease. *Nat Rev Neurol* 6:131–144.
10. Näslund J, et al. (1994) Relative abundance of Alzheimer A beta amyloid peptide variants in Alzheimer disease and normal aging. *Proc Natl Acad Sci USA* 91:8378–8382.
11. Grundke-Iqbal I, et al. (1986) Abnormal phosphorylation of the microtubule-associated protein tau (tau) in Alzheimer cytoskeletal pathology. *Proc Natl Acad Sci USA* 83:4913–4917.
12. Wolfe MS (2003) The secretases of Alzheimer's disease. *Curr Top Dev Biol* 54:233–261.
13. Portelius E, et al. (2010) Mass spectrometric characterization of brain amyloid beta isoform signatures in familial and sporadic Alzheimer's disease. *Acta Neuropathol* 120:185–193.
14. Iwata N, et al. (2000) Identification of the major Abeta1-42-degrading catabolic pathway in brain parenchyma: Suppression leads to biochemical and pathological deposition. *Nat Med* 6:143–150.
15. Qiu WQ, et al. (1998) Insulin-degrading enzyme regulates extracellular levels of amyloid beta-protein by degradation. *J Biol Chem* 273:32730–32738.
16. Hemming ML, Selkoe DJ (2005) Amyloid beta-protein is degraded by cellular angiotensin-converting enzyme (ACE) and elevated by an ACE inhibitor. *J Biol Chem* 280:37644–37650.
17. Mawuenyega KG, et al. (2010) Decreased clearance of CNS beta-amyloid in Alzheimer's disease. *Science* 330:1774.
18. Gram Schjoldager KT-B, et al. (2010) O-glycosylation modulates proprotein convertase activation of angiopoietin-like protein 3—possible role of polypeptide GalNAc-transferase-2 in regulation of concentrations of plasma lipids. *J Biol Chem* 285:36293–36303.
19. Semenov AG, et al. (2009) Processing of pro-brain natriuretic peptide is suppressed by O-glycosylation in the region close to the cleavage site. *Clin Chem* 55:489–498.
20. Portelius E, et al. (2007) Characterization of amyloid beta peptides in cerebrospinal fluid by an automated immunoprecipitation procedure followed by mass spectrometry. *J Proteome Res* 6:4433–4439.
21. Portelius E, Westman-Brinkmalm A, Zetterberg H, Blennow K (2006) Determination of beta-amyloid peptide signatures in cerebrospinal fluid using immunoprecipitation-mass spectrometry. *J Proteome Res* 5:1010–1016.
22. Portelius E, et al. (2010) A novel Abeta isoform pattern in CSF reflects gamma-secretase inhibition in Alzheimer disease. *Alzheimers Res Ther* 2:7.
23. Cook JJ, et al. (2010) Acute gamma-secretase inhibition of nonhuman primate CNS shifts amyloid precursor protein (APP) metabolism from amyloid-beta production to alternative APP fragments without amyloid-beta rebound. *J Neurosci* 30:6743–6750.
24. Portelius E, et al. (2009) Identification of novel APP/Abeta isoforms in human cerebrospinal fluid. *Neurodegener Dis* 6:87–94.
25. Riboni L, et al. (1986) Natural occurrence of ganglioside lactones. Isolation and characterization of GD1b inner ester from adult human brain. *J Biol Chem* 261:8514–8519.
26. Mirgorodskaya E, Roepstorff P, Zubarev RA (1999) Localization of O-glycosylation sites in peptides by electron capture dissociation in a Fourier transform mass spectrometer. *Anal Chem* 71:4431–4436.
27. Nilsson J, et al. (2009) Enrichment of glycopeptides for glycan structure and attachment site identification. *Nat Methods* 6:809–811.
28. Smythe C, Caudwell FB, Ferguson M, Cohen P (1988) Isolation and structural analysis of a peptide containing the novel tyrosyl-glucose linkage in glycogenin. *EMBO J* 7:2681–2686.
29. Aon MA, Curtino JA (1985) Protein-bound glycogen is linked to tyrosine residues. *Biochem J* 229:269–272.
30. Zarschler K, et al. (2010) Protein tyrosine O-glycosylation—a rather unexplored prokaryotic glycosylation system. *Glycobiology* 20:787–798.
31. Tabak LA (2010) The role of mucin-type O-glycans in eukaryotic development. *Semin Cell Dev Biol* 21:616–621.
32. Fukuda M, Lauffenburger M, Sasaki H, Rogers ME, Dell A (1987) Structures of novel sialylated O-linked oligosaccharides isolated from human erythrocyte glycophorins. *J Biol Chem* 262:11952–11957.
33. Canis K, et al. (2010) The plasma von Willebrand factor O-glycome comprises a surprising variety of structures including ABH antigens and disialosyl motifs. *J Thromb Haemostasis* 8:137–145.
34. Molander-Melin M, et al. (2005) Structural membrane alterations in Alzheimer brains found to be associated with regional disease development; increased density of gangliosides GM1 and GM2 and loss of cholesterol in detergent-resistant membrane domains. *J Neurochem* 92:171–182.
35. Barrier L, et al. (2007) Genotype-related changes of ganglioside composition in brain regions of transgenic mouse models of Alzheimer's disease. *Neurobiol Aging* 28:1863–1872.
36. Schnaar RL (2010) Brain gangliosides in axon-myelin stability and axon regeneration. *FEBS Lett* 584:1741–1747.
37. Inoue S, Iwasaki M (1978) Isolation of a novel glycoprotein from the eggs of rainbow trout: Occurrence of disialosyl groups on all carbohydrate chains. *Biochem Biophy Res Commun* 83:1018–1023.
38. Finne J (1982) Occurrence of unique polysialosyl carbohydrate units in glycoproteins of developing brain. *J Biol Chem* 257:11966–11970.
39. Galuska SP, et al. (2010) Synaptic cell adhesion molecule SynCAM 1 is a target for polysialylation in postnatal mouse brain. *Proc Natl Acad Sci USA* 107:10250–10255.
40. Suzuki M, Angata K, Nakayama J, Fukuda M (2003) Polysialic acid and mucin type O-glycans on the neural cell adhesion molecule differentially regulate myoblast fusion. *J Biol Chem* 278:49459–49468.
41. Mühlenhoff M, Oltmann-Norden I, Weinhold B, Hildebrandt H, Gerardy-Schahn R (2009) Brain development needs sugar: The role of polysialic acid in controlling NCAM functions. *Biol Chem* 390:567–574.
42. Gustafson DR, Skoog I, Rosengren L, Zetterberg H, Blennow K (2006) Cerebrospinal fluid-amyloid 1-42 concentration may predict cognitive decline in older women. *J Neurol Neurosurg Psychiatry* 78:461–464.
43. Brown MS, Ye J, Rawson RB, Goldstein JL (2000) Regulated intramembrane proteolysis: A control mechanism conserved from bacteria to humans. *Cell* 100:391–398.
44. May P, Bock HH, Nimpf J, Herz J (2003) Differential glycosylation regulates processing of lipoprotein receptors by gamma-secretase. *J Biol Chem* 278:37386–37392.
45. Maryon EB, Molloy SA, Kaplan JH (2007) O-linked glycosylation at threonine 27 protects the copper transporter hCTR1 from proteolytic cleavage in mammalian cells. *J Biol Chem* 282:20376–20387.
46. Portelius E, et al. (2011) A novel pathway for amyloid precursor protein processing. *Neurobiol Aging* 32:1090–1098.

BIOCHEMISTRY

CHEMISTRY